JOURNAL OF Applied Polymer SCIENCE

Morphology and Mechanical Properties of PET/PE Blends Compatibilized by Nanoclays: Effect of Thermal Stability of Nanofiller Organic Modifier

M. Yousfi,[1,2] J. Soulestin,[1,2] B. Vergnes,[3] M. F. Lacrampe,[1,2] P. Krawczak[1,2]

[1]Ecole des Mines de Douai, Department of Polymers and Composites Technology & Mechanical Engineering, 941 Rue Charles Bourseul, BP 10838, 59508 Douai Cedex, France

[2]Université Lille Nord de France, 59000 Lille, France

[3]MINES ParisTech, CEMEF, UMR CNRS 7635, BP 207, 06904 Sophia-Antipolis Cedex, France

Correspondence to: J. Soulestin (E-mail: jeremie.soulestin@mines-douai.fr)

ABSTRACT: Poly(ethylene terephtalate)/poly(ethylene) (PET/PE) blends (80/20 wt %) were prepared by melt-extrusion and compatibilized by addition of nanoclays. Two commercially available organically modified montmorillonites (Cloisite© 10A and 30B) were chosen as reference and a third one was specially organomodified at lab scale with a thermally stable phosphonium surfactant using conventional cationic exchange reaction. The size of the dispersed polymer phase (PE droplets) and the ductility of the blends depend more on the thermal stability of the surfactant of the organomodified clay than on the enthalpic interactions between the blend components and the surfactants used for the modification of the clays. The highest mechanical properties (yield stress and elongation at break) and the better compatibilization efficiency (smallest dispersed PE droplets) were observed in the presence of phosphonium organomodified montmorillonite compared to other less thermally stable commercial organoclays. The analysis of the thermal stability, morphology, and mechanical properties of PET/PE blends containing the surfactants alone in the absence of clay made it possible to evidence separately the effects of the surfactant and of the nanofiller. The role of the surfactant as compatibilization agent was demonstrated. In the absence of nanofiller, the finest morphological and highest ductility were again obtained with the phosphonium surfactant which is the most thermally stable. © 2012 Wiley Periodicals, Inc. J. Appl. Polym. Sci. 000: 000–000, 2012

KEYWORDS: blends; compatibilization; clay; surfactants; mechanical properties

Received 25 May 2012; accepted 6 August 2012; published online
DOI: 10.1002/app.38450

INTRODUCTION

In the last decade, many works have focused on the improvement of the morphology and interfaces of polymer blends using organomodified clays as compatibilizers.[1–5] Most commercial organoclays are functionalized by a quaternary ammonium surfactant, which has an affinity with one or both of the blends components. In the particular case of polymer matrix/organoclay systems, many authors have reported the effect of thermal stability of the clay organomodifier on the dispersion of the organoclay nanoplatelets in the matrix and the resulting mechanical properties.[6–11] To our knowledge, no study has addressed the effect of surfactant thermal degradation on the morphology and induced mechanical properties of immiscible polymer blends yet.

Nonetheless, the surfactants degradation and their decomposition products have to be taken into account to understand how the partially degraded surfactants and the released chemicals may affect the polymer blend properties. Regarding the thermal stability of surfactants, using regular commercial organoclays as compatibilizers may be suitable for polymer blends prepared with a low processing temperature. However, for most polymers which require high melt processing temperatures (e.g., poly(ethylene terephtalate), polyamide, and polycarbonate), the thermal stability of the organic component of the modified clay and its influence on the polymer blend properties are issues that must be considered.

Cui et al.[12] reported that the traditional ammonium-based organic surfactants used to modify commercial organoclays show measurable thermal degradation at temperatures as low as 180°C and that significant degradation occurs just above this temperature. Gelfer et al.[13] claimed that the loss of properties in polymer-organoclay nanocomposites can be related to the desorption and/or thermal degradation of surfactant molecules in

Applied Polymer SCIENCE

Table I. Modifier Specifications for Used Commercial Montmorillonites

Commercial name	Cloisite© 10A	Cloisite© 30B
Modifier chemical name	2MBHT	MHT2EOH
Anion	Chloride	Chloride
Modifier concentration (wt %)	39	30
Basal spacing (nm)	1.92	1.85

ammonium modified organoclays, which takes place at 180°C. Fornes et al.[14] suggested that the by-products formed from the breakdown of the organic surfactant might lead to degradation of the polymer during melt processing of polyamide 6 nanocomposites, which greatly influences polymer matrix characteristics. Thus, it would decrease the desired properties of organoclay compatibilized blends. Compatibilization of poly(ethylene terephtalate)/low density polyethylene (PET/LDPE) blends with organoclay without thermal degradation of the organomodifier during processing would require an organoclay being thermally stable at temperatures higher than the processing temperatures (~270°C). Phosphonium[8,15–17] or immidazolium-based surfactants[10,18–23] would be worth being considered for this purpose.[11]

This article reports the preparation of a new thermally stable organosilicate, for compatibilization of immiscible PET/PE blends. For this purpose, an organic modifier surfactant with three phenyl components as functional group and a phosphonium cation was chosen for its ability to satisfy two major conditions: (1) existence of a functional group more compatible with PET matrix than with the PE dispersed phase; (2) existence of a cationic group which is thermally stable at the blend melt-mixing temperature (≈ 270°C). For comparison, PET/PE blends were also prepared using commercial organoclays. Thermal stability, morphology, and tensile mechanical properties of PET/PE nanocomposites were evaluated. Then, the effect of surfactant was studied separately in the absence of montmorillonite platelets to assess the contribution of the surfactant alone on the thermal stability, morphology, and mechanical properties of the blends.

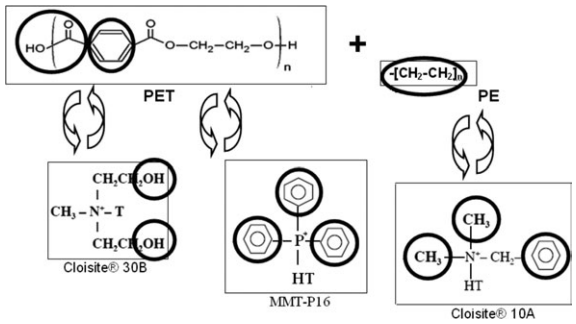

Figure 1. Degree of compatibility between the clay organomodifiers (surfactants) and each polymer.

EXPERIMENTAL

Materials

Low density PE Riblene FL 20 (density 0.921 g cm^{-3}, melt flow index 2.2 g/10 min [190°C, 2.16 kg], melting temperature 109°C) was supplied by Polimeri Europa (Italy). PET pellets (density 1.4 g cm^{-3}, intrinsic viscosity 0.98 dL g^{-1} at 30°C) was supplied by Acordis (The Netherlands). The clays were organomodified montmorillonites (OMMT) provided by Southern Clay Products (Gonzales, TX). They are sodium montmorillonite (Na^{+}-MMT) substituted with quaternary ammonium chloride, respectively modified by 2MBHT (dimethyl, benzyl, hydrogenated tallow) for Cloisite® 10A (C10A), and MHT2EOH (methyl, tallow, bis-2-hydroxyethyl) for Cloisite® 30B (C30B). Hydrogenated tallow (HT) is composed of around 65% C18, 30% C16, and 5% C14 (Table I). The surfactants of C30B and C10A have a special affinity with PET, and both PET and polyolefins, respectively (Figure 1).

The organic modifiers used in the preparation of PET/PE/surfactant blends were benzyldimethylhexadecyl ammonium

Table II. Chemical Structure, Melting Point, Molecular Weight, and Suppliers of Surfactants Used

Product	Chemical structure	Chemical name	Melting point[a] (°C)	Supplier
S10A	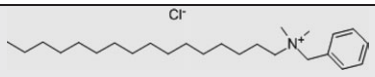	Benzyldimethylhexadecyl ammonium chloride	54–58	Acros
S30B	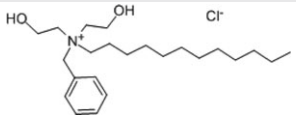	Benzylbis(2-hydroxyethyl) dodecyl ammonium chloride	113–120	Sachem Europe
P16	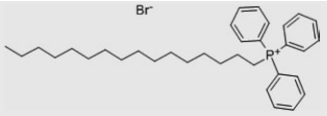	(1-Hexadecyl)triphenyl phosphonium bromide	100–105	Alpha Aesar

[a]Data provided by the supplier.

chloride from Acros Organics (Belgium), benzylbis (2-hydroxyethyl) dodecyl ammonium chloride from Sachem Europe (The Netherlands), and hexadecyltriphenyl phosphonium bromide from Alfa Aesar (Germany). They are referenced as S10A and S30B for surfactants corresponding to C10A and C30B, respectively. Phosphonium surfactant is referenced as P16 and the corresponding "home-treated" modified clay as MMT-P16. The chemical structures and melting temperatures of all surfactants used are listed in Table II.

Preparation of a New Thermally Stable Organoclay

The standard cation exchange reaction method was used to replace the sodium cations present in the interlayer space of Na^+-MMT with quaternary phosphonium cations (denoted as P16) to obtain a new organomodified clay (MMT-P16) (Figure 2). The amount of surfactant used for the cationic-exchange reaction is calculated according to eq. (1):

$$(92/100) \times 10\,\text{g}\,(\text{for clay}) \times 1.2 - (X/M_w\,\text{of surfactant}) \times 1 \times 1000 \quad (1)$$

where X and M_w represent the amount and the weight-average molecular weight of surfactant used, respectively, 92/100 represents the cation-exchange capacity (CEC) of 92 mEq/100 g of MMT, and 1.2 (>1) indicates the excess amount of the surfactant used.

Ten grams of MMT with a CEC value of 92 mEq/100 g were stirred in 400 mL distilled water (beaker A) at room temperature for 4 h. A separate solution was prepared by mixing an excess of surfactant salt (6.3 g) with other 100 mL of distilled water (beaker B) at room temperature, under magnetic stirring for 1 h. On the other hand, the MMT suspension (beaker A) was gradually heated to 80°C and mechanically stirred in a 1-L reactor for 2 h. Beaker B was then added at a slow rate under agitation to the MMT suspension (beaker A). The prepared mixture remained agitated for 5 h at 80°C. P16-exchanged clay solution was then filtered with a Buchner funnel. Purified products were obtained by sequential washing and filtering of the samples, at least three times to remove any excess of phosphonium ions. The product was then dried in vacuum overnight at 45°C and ground into powder to get the MMT-P16 organoclay. The grafting content of MMT-P16 was evaluated at 42 wt % from thermo-gravimetric analysis (TGA) test.

Preparation of PET/PE/OMMT and PET/PE/Surfactant Blend Samples

Before extrusion, PET pellets were dried in a vacuum oven overnight at 80°C.

PET/PE (80/20 wt %) and PET/PE/OMMT (80/18/2 wt %) blends were prepared using a conical co-rotating twin screw micro-compounder (Minilab Rheomex CTW5, Thermo Scientific, Germany). Blends of each composition were prepared under the same mixing conditions. The rotational speed was set-up at 50 rpm, corresponding to an average shear rate of 50 s^{-1}.[24] The temperature was fixed to 270°C and the residence time was 62 s.

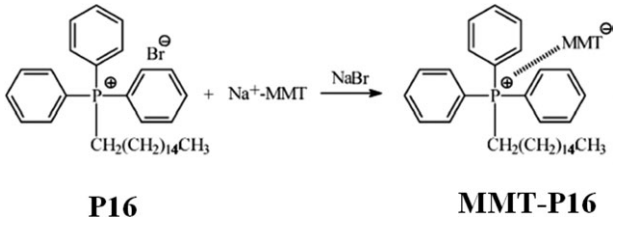

Figure 2. Schematic of cationic exchange reaction between sodium cations of native montmorillonite Na^+-MMT and phosphonium cations of P16 surfactant resulting in MMT-P16 organoclay.

All surfactants were added to the neat polymer blends as received, in the form of solid powders. The powder was previously crushed in a mortar, then added to the PET and PE pellets at a concentration of 0.6 wt %. The concentration of PE and PET was 19.4 wt % and 80 wt %, respectively. Powder and pellets were mixed at room temperature using a spatula and introduced in a vacuum oven at 100°C for 30 min, until the powder was completely softened and uniformly coated on the PET and PE pellets. The PET/PE/surfactant (80/19.4/0.6 wt %) blends were then prepared using the same processing conditions as that used to prepare PET/PE/OMMT blends.

For scanning electron microscopy (SEM) characterization, samples were injection-molded using the injection machine (Haake Minijet, Thermo Scientific, Germany) coupled to the micro-compounder. The temperatures of the cylinder and the mold were 280°C and 80°C, respectively. The pressure applied was 90 MPa for 15 s.

For X-ray diffraction (XRD) characterization, disks of 40 mm diameter and 1 mm thickness were compression-molded in a hot press (Dolouets 383, France) from blends pellets obtained by extrusion and pre-dried at 80°C for 4 h in a vacuum oven. A compression pressure of 11 MPa for 3 min and a temperature of 270°C were applied. After cooling to room temperature, the mold was taken out of the press and opened.

Characterization

Blends morphologies were examined by SEM using a Hitachi S4300 SE/N (Japan) instrument at accelerating voltage of 15 kV and a probe current of 130 pA. SEM photographs of the PET/PE and PET/PE/OMMT blends were made from injection-molded parts fractured in liquid nitrogen and then coated with gold to avoid charging on the fracture surface. To quantitatively analyze the morphology of the fractured surface of the samples, the average PE domain diameters and their polydispersities were measured by means of an image analysis software (ImageJ©, USA).

XRD curves were recorded on a horizontal diffractometer (D8 Bruker, Germany) operating at 40 kV and 40 mA with a beam consisting of CoKα radiation (λ = 1.78897 Å). Data were collected in the 2θ region 2–10°, with a step size of 0.004° and a counting time of 30 s per step. The basal spacing of the OMMT before and after intercalation was estimated from the position of d_{001} peak in the XRD diffractogram, according to the Bragg equation $n\lambda = 2d \sin\theta$, where d is the spacing between silica layers of the clay, λ the wavelength of X-ray, θ the reflection

Table III. Group Contributions to the Cohesive Energy and Molar Volume Used to Estimate the Solubility Parameter for Clay Organo-Modifiers (data taken from Fedors[27])

Group	E_{coh} (J mol^{-1})	V_m (cm^3 mol^{-1})
—CH_3	4707	33.5
—CH_2—	4937	16.1
—OH	29 790	10.0
Phenyl	31 924	71.4
N	4184	−9.0
P	9420	5.2

angle of X-ray on the silica layer, and n is a whole number which represents the order of diffraction, taken 1 in our calculations.

Tensile tests were carried out according to ISO 527 on a tensile machine (Instron 5585 H, USA) at a cross-head speed of 10 mm/min and at 23°C ± 2°C and 50% ± 5% relative humidity. The mechanical properties (mainly the elongation at break, ε_R) were determined from the recorded load–displacement curves. A minimum of five specimens was tested for each reported value.

TGA was carried out under air (Model Pyris TGA 7, Perkin Elmer, USA). Scans were recorded at a heating rate of 20°C min^{-1} over the temperature range from 30 to 700°C. For isothermal experiments, the temperature used was 270°C.

Calculation of Solubility Interaction Parameters and Surface Tensions of PET, PE, and Organoclay Modifiers

Because of large solubility parameter differences, most polymer blends are immiscible resulting in poor interfacial adhesion. The addition of organoclays tends to refine the morphology of immiscible blends, one of the main reasons being the interfacial tension decrease induced by the organoclays.[25] Therefore, the interaction characteristics of the organoclays used in this study are essential. Surface tension (γ) of each surfactant was deduced from its solubility parameter (δ) according to the empirical relationship proposed by Van Krevelen [eq. (2)].[26]

$$\gamma = 0.75 \times (\delta)^{4/3} \quad (2)$$

The solubility parameter (δ) was calculated on the basis of the contribution of each functional group (Table III) and each fragment of the parent structure to the cohesive energy (E_{cohi}) and molar volume (V_{mi})[27] [eq. (3)]:

$$\delta = \left(\frac{\sum E_{cohi}}{\sum V_{mi}}\right)^{1/2} \quad (3)$$

For the polymers (PET and PE), solubility parameters at room temperature[28,29] and surface tension at room temperature are used.[21] All the calculated parameters are reported in Table IV.

The solubility parameter of S10A (C10A surfactant) at 20°C is close to the one of PE, meaning that these two components are compatible. The solubility parameter of S30B (C30B surfactant) is the same as that of PET, indicating good surfactant/polymer compatibility. The solubility parameter of MMT-P16 modifier lies between the solubility parameters of PE and PET, which suggests that it is compatible with both polymeric phases. Consequently, considering the relative solubility parameters of the surfactants and polymers, P16 (MMT-P16 surfactant) would theoretically be the best compatibilizer[31] among the three OMMT for the immiscible PET/PE blends (Figure 1).

RESULTS AND DISCUSSIONS

Thermal Stability of Organoclays

The thermal stability of organosilicates plays a critical role during compounding of PET/PE/OMMT blends, because the processing temperature is high (270°C). Hence, the thermal stability of commercial and "home-treated" OMMT was investigated by TGA, before their addition into PET/PE blends. The measurements were carried out under air because blends are compounded in such conditions in the extruder.

The weight loss curves of organosilicates between room temperature and 700°C are shown in Figure 3(a). As expected, for all organoclays, the extent of mass loss increases with increasing temperature. However, the rate of surfactant loss increases dramatically in the range 240–400°C. Gelfer et al.[32] noticed the same trend for similar OMMT. After a little surfactant loss between 100 and 200°C, the major weight loss began at 240°C and continued until 400°C. However, many authors suggest better stability of organoclays containing surfactants such as phosphonium[15–17] and immidazolium salts.[10,18–20] Most of these salts exhibit onsets of degradation often above 300°C. As shown in Figure 3(a), the decomposition onset temperature of C10A and C30B is 180°C and 230°C, respectively. These temperatures are much lower than that of blend processing. Degradation of the clay modifier is therefore highly probable in these conditions, especially in the case of C10A. Interestingly, in the case of MMT-P16 organoclay, the onset of degradation is above 280°C, higher than the melt extrusion temperature.

Isothermal TGA measurements were also performed in air [Figure 3(b)] to determine the surfactant mass loss at 270°C (extrusion temperature of PET/PE blends). A temperature ramp of

Table IV. Solubility Parameter and Surface Tension of Clay Organo-Modifiers and Polymers Used

Component	Solubility parameter[a] at 20°C (J cm^{-3})$^{0.5}$	Surface tension[b] at 20°C (mN m^{-1})	Molecular weight[c] (g mol^{-1})
S10A	17.5	34.1	396.1
S30B	21.5	44.8	400.1
P16	19.3	38.8	567.6
PET	21.5	44.0	-
PE	16.4	33.0	-

[a]Calculated from eq. (1) for surfactants; from Hansen and Wallstrom[28] for polymers.
[b]Calculated from eq. (2) for surfactants; from Wu[30] for polymers.
[c]Data provided by the supplier

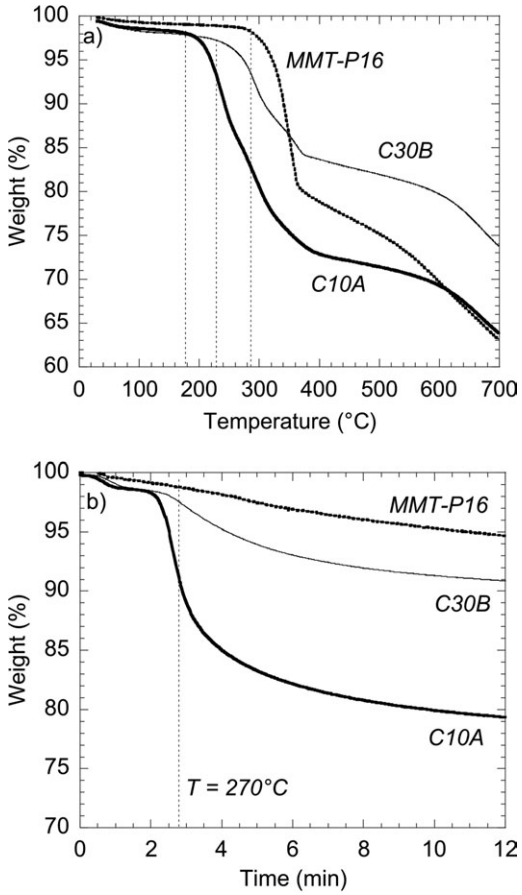

Figure 3. TGA curves under air atmosphere with a scanning rate of 20°C min^{-1} (a) and weight loss kinetics at 270°C under air of organoclays C10A, C30B, and MMT-P16 (b). Between room temperature and 270°C, the heating rate was 100°C min^{-1}.

100°C per minute was applied to jump from room temperature to 270°C. Thus, in less than 3 min, the mass loss of C30B and MMT-P16 is low (< 3%) and mainly due to the presence of moisture. In contrast, for C10A, before reaching 270°C a loss of about 10% is observed. Once the temperature of 270°C is reached, the mass loss rate decreases with time and then tends to stabilize after about 10 min. After 12 min, the mass loss is 5, 10, and 20% for MMT-P16, C30B, and C10A, respectively. This confirms that MMT-P16 is more thermally stable than C30B and much more than the unstable C10A.

It is worth mentioning that, on the basis of XRD and TGA measurements performed at different temperatures on different organoclays, Shah et al.[33] claimed that the mass of surfactant lost during melt processing of nanocomposites was found to be greater than during TGA of organoclays (in the absence of polymer). This could be attributed to the high solubility of the degradation products (predominantly α-olefins) in the polymer matrix, thus facilitating an easier removal of these by-products from the organoclay by extrusion as compared to TGA where the degradation products leave by evaporation. Consequently, although conditions of TGA measurements do not match those of the melt-extrusion process, TGA analysis provides relevant information on the level of possible degradation of organoclays.

Interlayer Spacing in Neat Organoclays and PET/PE/OMMT Blends

Figure 4 shows the XRD patterns of Na^+-MMT and the "home-treated" organoclay prepared in our laboratory using phosphonium surfactant (P16). The interlayer spacing of Na^+-MMT, calculated from the reflection at $2\theta = 8.88°$, is 1.16 nm. After the ion-exchange reaction with phosphonium salt, reflection of the clay shifts to a new position at $2\theta = 5.4°$ ($d = 1.90$ nm). This means that the basal spacing increased significantly, providing evidence that surfactant intercalation has occurred. This result corroborates other literature reports.

Figure 5 shows the XRD patterns of neat C10A, C30B, MMT-P16 organoclays and the corresponding PET/PE/OMMT blends. The primary (d_{001}) diffraction peak of neat commercial organoclays used is located around $2\theta \approx 5.5°$, which corresponds to an interlayer spacing (d-spacing) of 1.87 nm. Upon addition of organoclay to PET/PE blend, this XRD peak shifts to lower angles, indicating the increase in interlayer spacing by polymer intercalation. For C30B and C10A, the average distance between the platelets is then 3.23 and 3.12 nm, respectively, instead of 1.87 nm before intercalation. However, in the case of MMT-

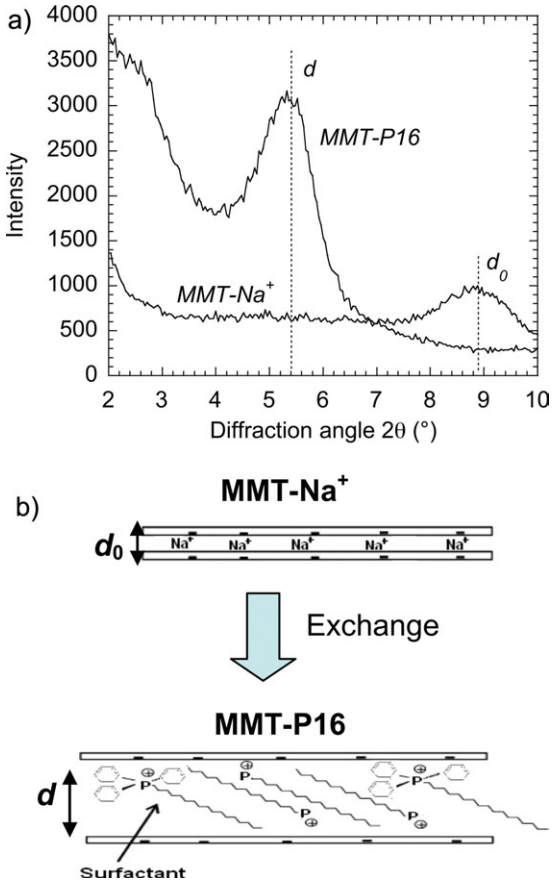

Figure 4. (a) XRD diffractograms of native sodium montmorillonite Na^+-MMT and phosphonium organomodified MMT-P16 clay. (b) Schematic of phosphonium surfactant intercalation in montmorillonite platelets. [Color figure can be viewed in the online issue, which is available at wileyonlinelibrary.com.]

Applied Polymer SCIENCE

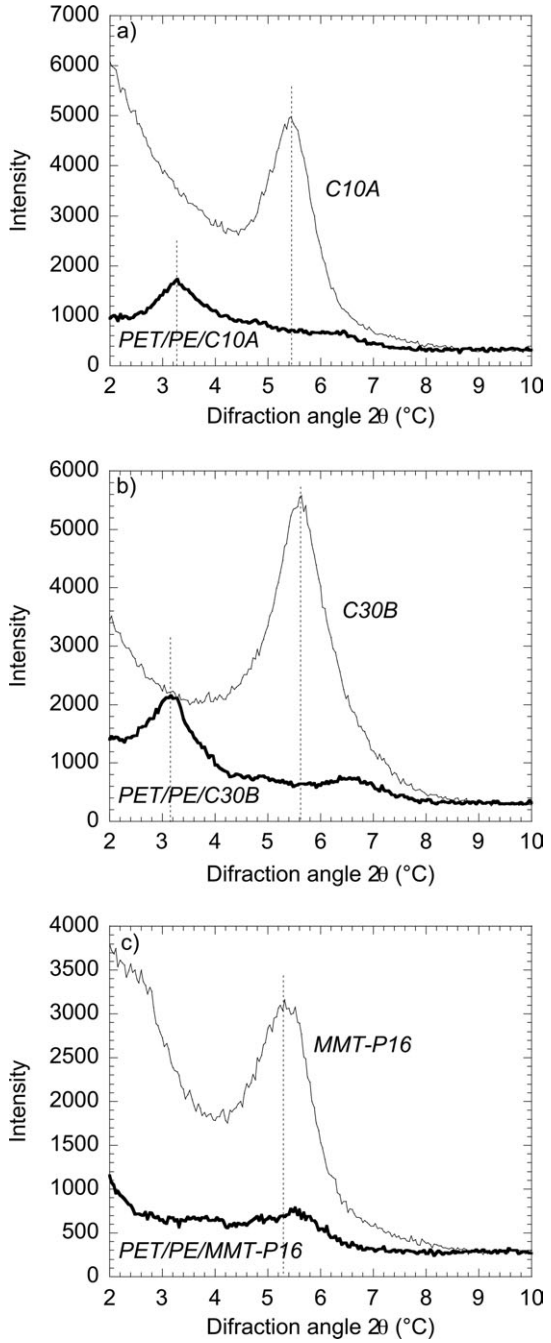

Figure 5. XRD patterns for the organoclays and the PET/PE/OMMT blends. (a) C10A, (b) C30B, (c) MMT-P16.

P16, no peak is observed. Moreover, a shallow diffraction peak located around $2\theta = 6.4°$ (d-spacing: 1.60 nm) for C10A and C30B and $2\theta = 5.5°$ (d-spacing: 1.87 nm) for MMT-P16 is also observed. This second diffraction peak may be ascribed to the second order diffraction (d_{002}).

The XRD analysis attests the formation of an intercalated structure for all the blends with few exfoliation. As the aim of this work is to evaluate the influence of the surfactant "grafted" at clay surface, and not the dispersion of clay, this result is important. Indeed, the intercalated structure is similar for all the blends; the viscosities of the polymer phases are modified, due to the presence of the organoclays, in a similar way. Therefore, any blends morphology modification will be mainly controlled, as commonly accepted,[25] by interfacial tension changes and organoclays localization related to the different surfactants at the tactoids surface.

Morphology of PE Domains

Figure 6 shows the cryofractured surfaces of PET/PE blends with and without 2 wt % of OMMT. The sections observed are perpendicular to the injection flow (transverse direction). As already highlighted on similar systems in an other paper,[31] considering the size of PE nodules in the PET/PE blends before and after addition of organoclays, the addition of 2 wt % of organoclay clearly induces a decrease of the PE droplet size for C30B and even more here for MMT-P16 (Figure 7). In the absence of clay, large diameters of PE domains are observed and the interface is clearly visible, which is typical of poor interfacial bonding. Actually, PE nodules are pulled out during the cryofracture, due to the weak interfacial adhesion between PET and PE, as attested by the presence of numerous holes. When C10A is used the morphology of the blend is similar to the one of neat PET/PE blend. The addition of C30B and MMT-P16 induces a significant change in the size and the size distribution of PE droplets, particularly for MMT-P16. This change of morphology indicates that the compatibility between PET and PE is greatly improved in the presence of MMT-P16. This "home-treated" OMMT leads to the highest decrease of the PE droplet size and to the highest size homogeneity, whereas C30B is in comparison less efficient. The average PE domain size in PET/PE blend decreases from 8 μm to around 1.5 μm with the addition of 2 wt % of MMT-P16 and to 3.9 μm in the case of C30B [Figure 7(a)]. In the case of C10A, a limited effect is observed with a very slight change in the droplet size and an increasing scattering of the droplet size distribution. These results seem to be consistent with the values of surface tensions as already discussed.

Nevertheless, it is worth mentioning that considering the severe extrusion conditions (high temperature), the thermal stability of the organoclay surfactants could also influence the morphology of the blends. Therefore, another possible explanation of the observed trends is that blends morphology depends on surfactants thermal stability. When the thermal stability of the clay organomodifier increases, the morphology is finer and more homogeneous (Figure 8). MMT-P16 leads to a finer morphology because of its higher thermal stability. Taking this fact into account, the prediction of the effectiveness of clay compatibilization on the only basis of its initial affinity with the matrix and/or the dispersed phase estimated at room temperature is not so straightforward. Indeed, other parameters may interfere.

Usually, models based on processing conditions are used to predict the morphology of polymer blends. The morphology, described by the droplets diameter, is controlled by the interfacial tension between the phases, their viscosities, and the shear rate. Serpe et al.[34] proposed a model considering also the volume fraction of the components [eq. (4)]:

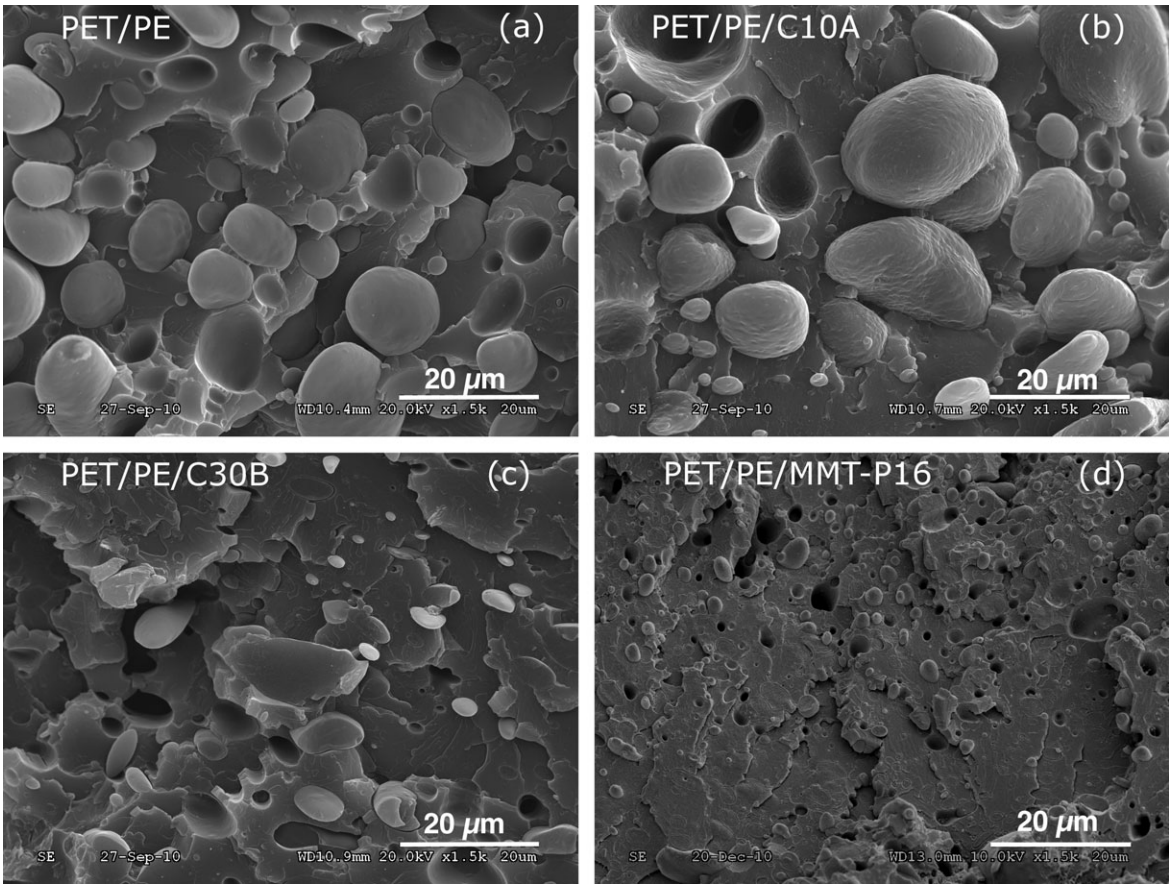

Figure 6. SEM micrographs of fracture surfaces of the PET/PE/OMMT blends (PET/PE/OMMT = 80/18/2 wt %).

$$D \approx \frac{\frac{4\Gamma_{PE/PET}}{\dot{\gamma}\eta_b}\left(\frac{\eta_d}{\eta_b}\right)^{\alpha}}{1-\left(4\times\Phi_{PE}\times\Phi_{PET}\right)^{0.8}} \quad (4)$$

where α is an experimental parameter, and has a value of nearly 0.84, which is positive if the viscosity ratio η_d/η_b is larger than one and negative otherwise. D is the droplet size, Γ the interfacial tension (at the processing temperature) between PET and PE, $\eta_{d,}$ the viscosity of the PE dispersed phase, η_b the viscosity of the blend, $\dot{\gamma}$ the shear rate and Φ the volume fraction. In the case of the studied blends, as the same processing conditions were used for all the blends, the shear rate is constant. Moreover, XRD analysis showed that the dispersion of organoclay is similar for all the blends (intercalated structure). Accordingly, its influence on the blend morphology will be comparable in all the cases. Consequently, shear rate and viscosity changes related to the dispersion of organoclay cannot explain the morphology changes which would be controlled essentially by interfacial tension changes. Furthermore, the influence of thermal degradation on the morphology must be taken into account. Actually, even if the values of solubility parameters and surface tensions at room temperature may give some indication of the efficiency of the added organoclay, the degradation of the surfactant during extrusion at high temperature may lead to a modification of the interfacial tension.[35] It also possibly induces some degradation of the polymers, chain breakage leading to viscosities changes resulting in viscosity ratio variations. Besides, interfacial tension, computed from the solubility parameters at room temperatures, is not totally representative of the interfacial tension at the processing temperature. In addition, the viscosities measured separately for each polymer are not representative of the viscosities during processing as it does not take into account for the degradation induced by the surfactant. Therefore, it appears that it is very difficult to predict, in the present study, the effect of the addition of organoclay on the morphology of a PET/PE blend using the Serpe model. This conclusion is also well-founded for any blend needing a processing temperature higher than the degradation temperature of any of its components.

Mechanical Properties of PET/PE/OMMT Blends

The mechanical behavior of the PET/PE blends with and without OMMT was characterized by uniaxial tensile tests. The stress–strain curves shown in Figure 9 represent one test for each composition. The addition of C10A has a negative effect on both yield stress and elongation at break. PET/PE blend is ductile ($\varepsilon_R > 80\%$) whereas PET/PE/C10A blend is clearly brittle ($\varepsilon_R < 10\%$). In contrast, the ductility is partially preserved upon addition of C30B ($\varepsilon_R \sim 40\%$) and MMT-P16 ($\varepsilon_R \sim 60\%$) whereas the yield stress increases by approximately 10% and 20%, respectively, compared to neat PET/PE. This trade-off in

Applied Polymer SCIENCE

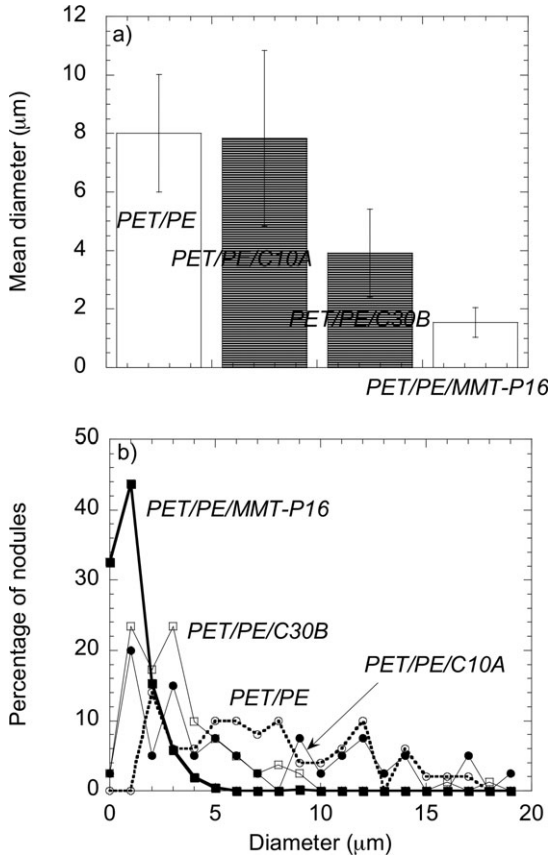

Figure 7. (a) Average PE droplets diameter and (b) particle size distribution for the different blends.

mechanical properties of PET/organoclay nanocomposites has been often reported in the literature.[36] Wang et al.[37] studied the influence of the mass concentration of DK2 organoclay (trade name for other OMMT, equivalent to C30B) on the mechanical properties of PET/DK2 nanocomposites, showing that the elongation at break and the impact resistance decrease with increasing concentration of clay. Kráčalík et al.[10] reported the effect of

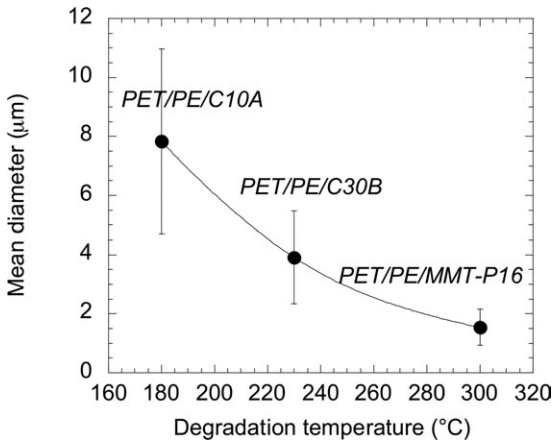

Figure 8. Variation of average PE droplets diameter versus onset of organoclay decomposition.

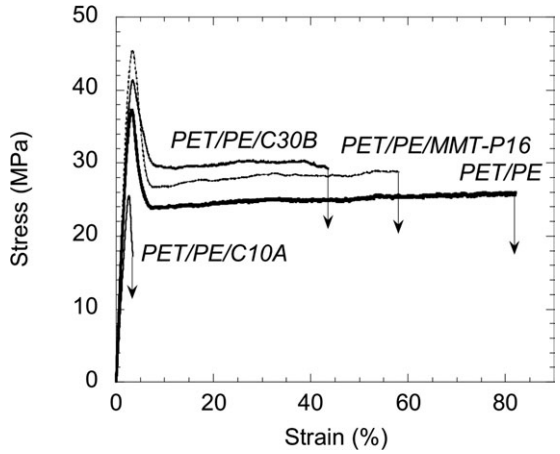

Figure 9. Stress–strain tensile curves for PET/PE and PET/PE/OMMT blends.

the addition of C10A and C30B on the mechanical and rheological properties of recycled PET as matrix. Although the Young's modulus increased upon addition of modified clay and although the latter was well dispersed in PET matrix, a drastic diminution of both elongation at break and tensile strength was observed (from 316.5% for neat PET to 5.1% and 19.2% in the presence of 5% of C10A and C30B, respectively). The authors ascribed these results to the thermal degradation of clay surfactant modifier during extrusion process. Indeed, the low thermal stability of these organoclays results in their chemical decomposition, either by nucleophilic substitution or by α,β elimination reaction mechanism[12,38] (Figure 10). Hofmann elimination occurs in the presence of a basic anion, such as hydroxide, which extracts a hydrogen atom from the β-carbon of the quaternary ammonium, yielding an olefinic and a tertiary amine group. Other products of degradation formed at high temperature (CO_2, aldehydes) may lead to the decrease of mechanical properties of PET matrix. In the present work, C10A is the most thermally unstable organoclay, which explains the brittle mechanical behavior of PET/PE/C10A compared to other blends. It is worth mentioning that although MMT-P16 organoclay is thermally stable at the extrusion temperature of PET/PE blends, it leads to a slight reduction in elongation at break.

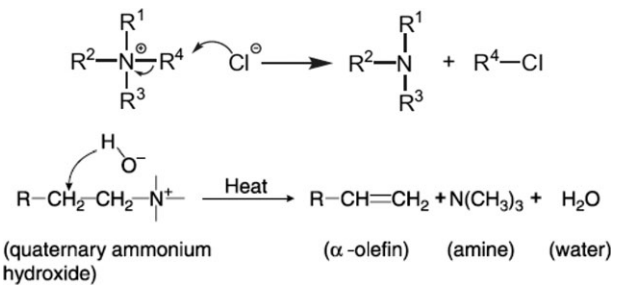

Figure 10. (a) Nucleophilic substitution leading to the decomposition of an ammonium surfactant (according to Ref. 12) and (b) scheme of α,β elimination (according to Ref. 39).

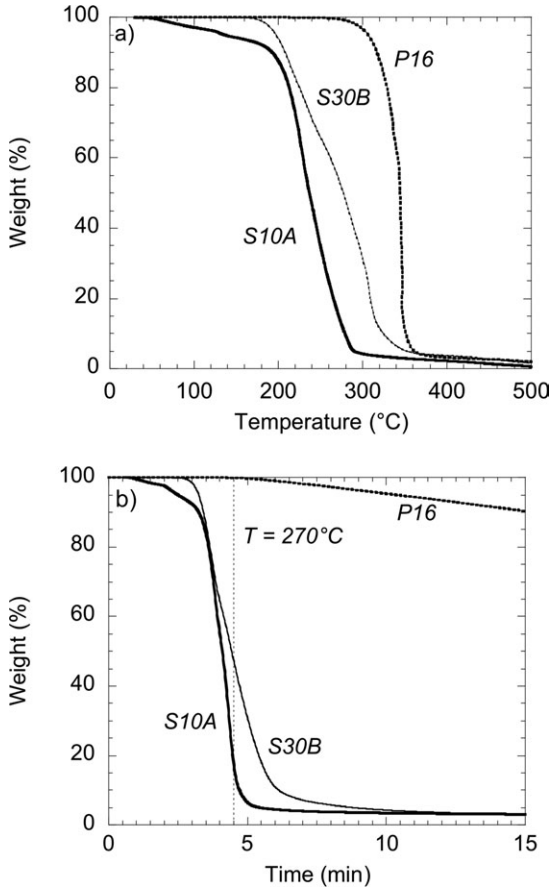

Figure 11. (a) TGA curves under air atmosphere with a scanning rate of 20°C min^{-1} and (b) weight loss kinetics at 270°C under air of surfactants S10A, S30B, and P16.

Sinha Ray et al.[1] reported similar trends on the ductility of PP-*g*-MA/PS (80/20 wt %) blends. Despite good thermal stability of the organoclay (because of the low extrusion temperature, 180°C) and a very good exfoliation of the organoclay in PP-*g*-MA matrix, the authors found a reduction of the elongation at break in the presence of clay. This may be ascribed to the unavoidable existence (even in well-dispersed nanocomposites) of few clay aggregates, which act as stress concentrations and crack initiation sites, as elongation at break is known to be very sensitive to materials defects.

Surfactant Effect on PET/PE Blend Properties in Absence of Montmorillonite

Thermal Stability of Surfactants. In order to separate the effect of the surfactant from that of the nanofiller, the thermal stability, morphology, and mechanical properties of PET/PE/surfactant blends were investigated in the absence of clay.

Figure 11(a) shows the weight loss curves of the surfactants used in this study. In the case of S10A, the first onset of degradation occurs at around 130°C, followed by a second onset of mass loss at 220°C. For S30B, the first onset occurs at 200°C, the second at 325°C. For P16, the first onset is at 300°C, the second at 345°C. Cervantes-Uc et al.[38] suggested that the low thermal stability of S10A is due to the presence of the benzyl group and aromatic structure, which was confirmed by the FTIR analysis of the evolved gases at the first stage of its thermal degradation. Despite the presence of three phenyl groups in its chemical structure, P16 surfactant is more stable because it contains a phosphonium group instead of an ammonium group.

As previously reported for clay-filled blends, isothermal TGA measurements were performed in air to determine the mass loss of the surfactant at 270°C [Figure 11(b)]. First, a temperature ramp of 60°C min^{-1} was applied from room temperature to 270°C. Thus, in less than 5 min, the mass loss of S10A and S30B reaches 92% and 62%, respectively. Meanwhile, the mass of P16 does not change. Once the temperature of 270°C is reached, an almost full decomposition of S10A and S30B surfactants occurs after 5 min, whereas the mass loss of P16 is limited to about 5% only. These results confirm the very good thermal stability of the P16 surfactant, which is much more thermally stable than the commercial S30B and S10A surfactants.

Morphology of PET/PE/Surfactant Blends. Figure 12 presents the SEM images of PET/PE blends with and without 0.6 wt % of surfactants. The average quantity of surfactant in most commercial OMMT is about 30 wt % (Table I). In this study, 2 wt % of clay were added, which corresponds to a surfactant concentration of 0.6 wt %.

As already mentioned in the case of PET/PE blends, the SEM micrograph [Figure 12(a)] reveals a two-phase morphology with larger PE domains embedded within the continuous PET matrix. In the case of PET/PE/surfactants blends, whatever the type of surfactant, the droplet size of the PE dispersed-phase decreases upon the addition of the surfactant acting as a regular compatibilizer. Indeed, whereas the droplet size in the PET/PE blend is 8 μm in the absence of surfactant, it decreases to 3.7 μm, 2.2 μm, and 1.4 μm upon addition of S10A, S30B, and P16 surfactants respectively [Figure 13(a)]. This reduction in droplet size may be due to the migration of surfactants chains to the boundary area between the two polymers, which adsorbed along the interface and interacted with the latter; this induces a decrease in the interfacial tension. Furthermore, the polydispersity of PE droplet sizes is sharply reduced in presence of P16 compared to S30B [Figure 13(b)]. The morphology with S30B surfactant is more homogeneous than that of S10A. These results are consistent with the ones obtained for the PET/PE/OMMT blends. This means that the presence of the clay does not directly affect the morphology; it is the surfactant, "grafted" at the surface of clay platelets and tactoids, that controls the blend structure.

As the effect of the surfactant on morphology may be ascribed to a decrease of the interfacial tension, it is possible to predict the surfactant efficiency based on its localization, by calculating the wetting coefficient. The wetting coefficient of surfactants (also frequently called spreading coefficient) was calculated using Harkins equation modified by Hobbs.[40] Indeed, this equation is generally used for ternary polymer blends,[41–43] compatibilized polymer blends,[44,45] blends containing block copolymer,[46,47] and ternary systems containing small molecules.[48] It seems to be relevant in this case, as surfactants are

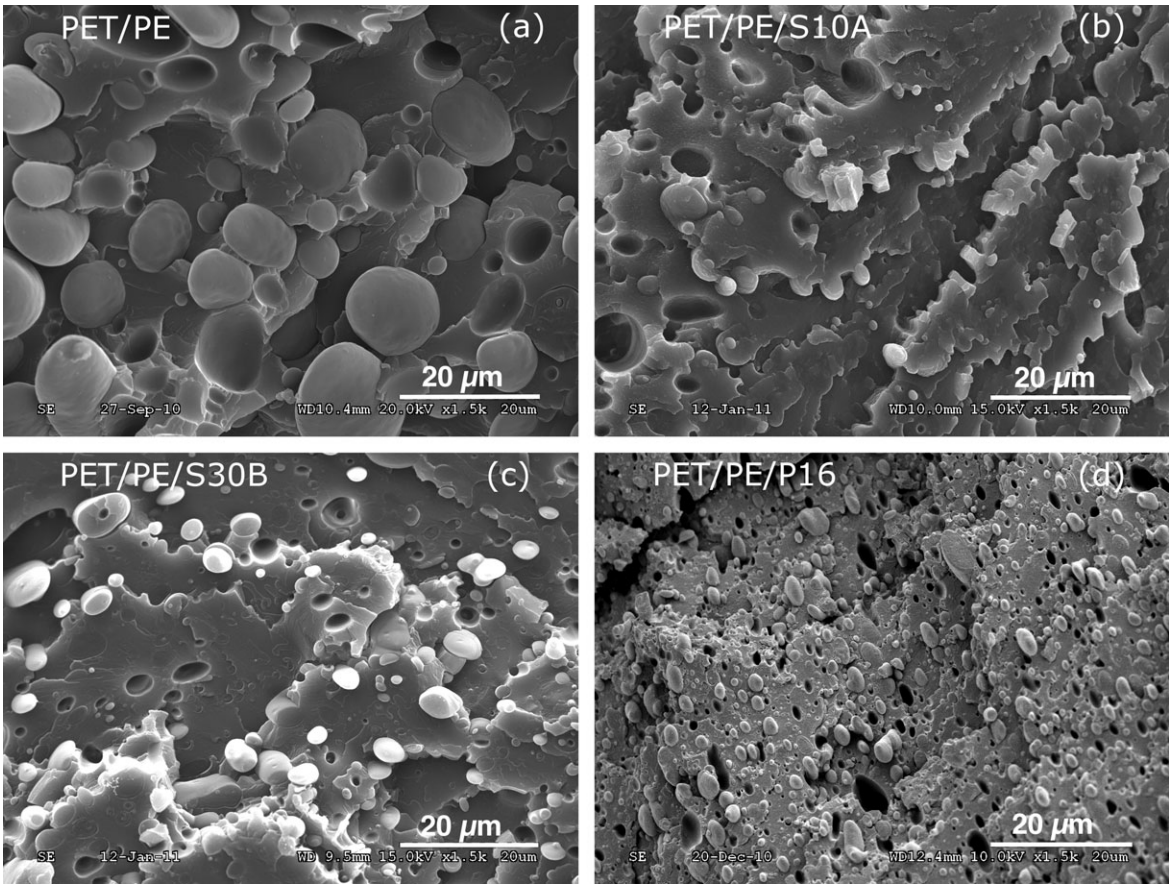

Figure 12. SEM micrographs of fracture surfaces of the PET/PE/surfactant blends (PET/PE/surfactant = 80/19.4/0.6 wt %).

low molecular weight molecules. The localization of the surfactants can be predicted from the spreading coefficients defined by eq. (5):

$$\lambda_{abc} = \gamma_{ac} - (\gamma_{ab} + \gamma_{bc}) \quad (5)$$

where γ_{ab} is the interfacial tension between a and b, γ_{ac} is the interfacial tension between a and c, γ_{bc} is the interfacial tension between b and c, and λ_{abc} is the spreading coefficient. The values of the different interfacial tensions were calculated from the surfactant and polymers surface energies (i.e., surface tensions, Table IV) using the Girifalco–Good equation.[49] The spreading coefficient λ_{abc} indicates the thermodynamic tendency of b to spread at the interface between a and c. In order to predict the equilibrium morphology, it is necessary to know a set of three spreading coefficients λ_{abc}, λ_{bac}, and λ_{acb}. If λ_{abc} is positive and the other two negative, b will be localized at the interface and thus lead to a maximum decrease of the interfacial tension between polymer phases. Table V gathers the values of the spreading coefficients in the case of the different surfactants.

Theoretically, S10A and P16 surfactant would therefore tend to be localized at the interface leading to highest decrease of interfacial tension, whereas S30B would be located in PET leading to lower refinement effect. Thus, the theoretical and experimental results are contradictory. Based on this observation, it appears that the difference in the polarities of the surfactants and its effect on interfacial tension is not sufficient to explain the effect of surfactants on the polymer blend morphology.

In the present study, it can be assumed that the nodule sizes also vary according to the thermal stability of the surfactants (Figure 8). It is important to note that the size of PE droplets is smaller when the surfactant is added alone in the absence of montmorillonite platelets (Figure 14). Various authors[12,38] have shown that the presence of clay enhances the degradation phenomenon of the surfactant. Indeed, the presence of oxygen in the montmorillonite structure (extracted from the crystal structure of the dehydroxylated MMT and present in the range of 31–45 wt %) may act as catalyst to enable the oxidative decomposition of surfactant at high temperature. Thus, in the absence of MMT, polymer chains have more time to access to and to be in contact with the surfactant; therefore the latter is more efficient in terms of morphology refinement.

Mechanical Properties of PET/PE/Surfactant Blends. Very few studies address the effect of the surfactant on the mechanical properties of immiscible polymer blends.[50] Most investigations on the role of surfactant have mainly focused on its effect on morphology. The addition of organoclays was found to induce a significant loss of ductility of PET/PE blends and this was

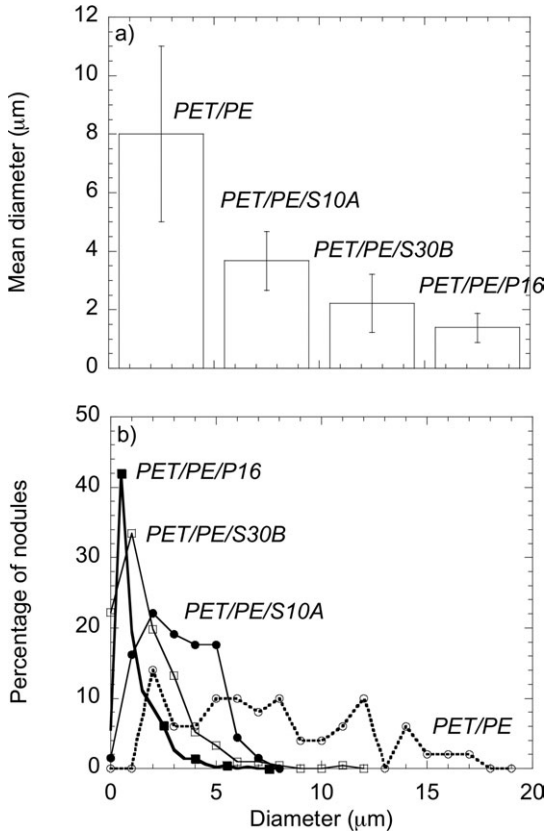

Figure 13. (a) Average PE droplets diameter and (b) particle size distribution for the different blends.

suspected not being caused by the presence of clay only. Analyzing the mechanical behavior of PET/PE blends with surfactant but without MMT aims at clarifying the origin of such variation in elongation at break.

Figure 15 shows the tensile stress–strain curves. Despite a clear improvement of the morphology of the blend, a ductility reduction is still observed upon addition of S10A and S30B surfactants. As already discussed, once the surfactant begins to decompose, the presence of oxygen may act as catalyst to enable the oxidative cleavage of alkenes to produce aldehydes at elevated temperatures.[38] The presence of aldehyde and other products of decomposition of the surfactant may produce undesired side reactions with PET matrix, as for instance the formation of a branched structure, resulting in a loss of ductility. All these phenomena are amplified in the presence of MMT. In addition

Table V. Spreading Coefficient λ for the Different Blends Containing Surfactants

Surfactant	λ_{1S2}	λ_{S12}	λ_{12S}
S10A	0.24	−0.29	−1.29
S30B	−0.40	−1.91	0.33
P16	0.39	−0.86	−0.72

Calculated from eq. (5) where PE corresponds to polymer 1 and PET to polymer 2.

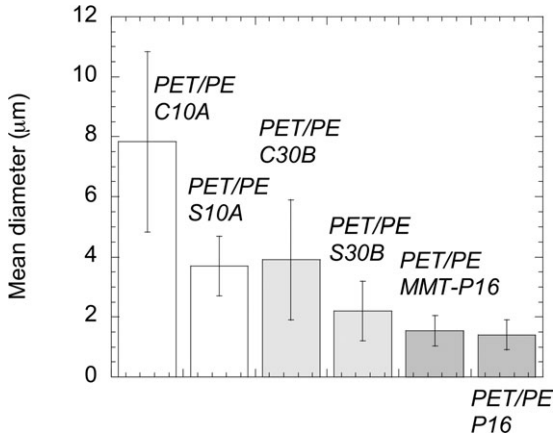

Figure 14. Comparison between average PE droplets diameter of different PET/PE/OMMT and corresponding PET/PE/surfactants blends.

to the aforementioned detrimental effect of few clay aggregates, this is the reason why the ductility of PET/PE/surfactant blends is better compared to the corresponding PET/PE/OMMT systems. Interestingly, the ductility of PET/PE/P16 blends is even improved compared to neat PET/PE blend since the phosphonium surfactant is very thermally stable and therefore less likely to generate harmful degradation products as in the case of other ammonium surfactants.

CONCLUSIONS

The efficiency of organoclays for compatibilizing an immiscible PET/PE blend and the induced mechanical properties were investigated as a function of the thermal stability of the clay organomodifier. Two commercial OMMT were considered as a reference (Cloisite® 10A and 30B). A new thermally stable organoclay was tailor-made, sodium montmorillonite being home-treated with a phosphonium surfactant using conventional cationic exchange reaction.

The mechanical properties and the morphological structures of organoclay-filled PET/PE blends depend more on the degradation onset temperature of clay organomodifiers than on the enthalpic interactions between the blend components and the

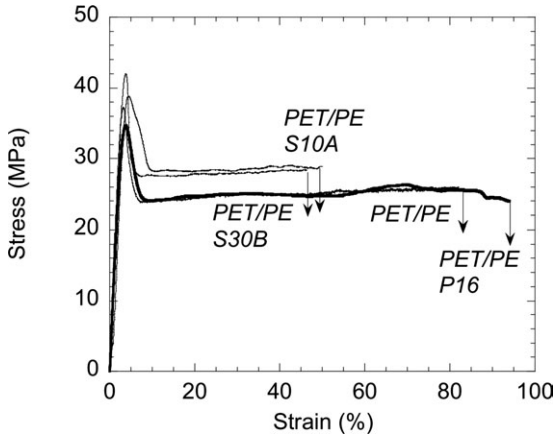

Figure 15. Stress–strain tensile curves for PET/PE and PET/PE/surfactant blends.

surfactants used for the modification of the clays. Indeed, the highest mechanical properties (yield stress and elongation at break) and the better compatibilization efficiency (smaller dispersed PE droplets) were observed in the presence of phosphonium organomodified montmorillonite compared to other less thermally stable commercial organoclays.

The analysis of the thermal stability, morphology, and mechanical properties of PET/PE/surfactant blends in the absence of clay made it possible to evidence separately the effects of the sole surfactant and of the nanofiller. The crucial role of the surfactant as compatibilization agent was demonstrated. The finest morphology and highest ductility were again obtained with the phosphonium surfactant which is the most thermally stable.

ACKNOWLEDGMENTS

This work was financially supported by the Carnot M.I.N.E.S Institute (France) in the frame of the "Nanostructure" project carried out by its Nanomines working group. The authors are indebted for valuable assistance provided by Damien Betrancourt and Laurent Charlet from Ecole des Mines de Douai in microscopy and extrusion experiments, respectively. The authors also gratefully acknowledge the International Campus on Safety and Intermodality in Transportation (CISIT), the Nord-Pas-de-Calais Region and the European Community (FEDER funds) for funding contribution to the micro-compounder and the scanning electron microscope.

REFERENCES

1. Sinha Ray, S.; Pouliot, S.; Bousmina, M.; Utracki, L. A. *Polymer* **2004**, *45*, 8403.
2. Sinha Ray, S.; Bousmina, M. *Macromol. Rapid Commun.* **2005**, *26*, 450.
3. Sinha Ray, S.; Bousmina, M. *Macromol. Rapid Commun.* **2005**, *26*, 1639.
4. Hong, J.; Namkung, H.; Ahn, K.; Lee, S.; Kim, C. *Polymer* **2006**, *47*, 3967.
5. Zhu, S. M.; Liu, Y.; Rafailovich, M.; Sokolov, J.; Gersappe, D.; Winesett, D. A.; Ade, H. Proceedings of the 218th Annual Conference of American Chemical Society, New Orleans, Louisiana, USA, August, **1999**, *218*, 431.
6. Stoeffler, K.; Lafleur, P. G.; Denault, *J. Polym. Degrad. Stab.* **2008**, *93*, 1332.
7. Kim, K. H.; Kim, K. H.; Huh, J.; Jo, W. H. Macromol. Res. **2007**, *15*, 178.
8. Costache, M. C.; Heidecker, M. J.; Manias, E.; Wilkie, C. A. *Polym. Adv. Technol.* **2006**, *17*, 764.
9. Kráčalík, M.; Mikešová, J.; Puffr, R.; Baldrian, J.; Thomann, R.; Friedrich, C. *Polym. Bull.* **2006**, *58*, 313.
10. Kráčalík, M.; Studenovský, M.; Mikešová, J.; Kovářová, J.; Sikora, A.; Thomann, R.; Friedrich, C. *J. Appl. Polym. Sci.* **2007**, *106*, 2092.
11. Kráčalík, M.; Studenovský, M.; Mikešová, J.; Sikora, A.; Thomann, R.; Friedrich, C.; Fortelný, I.; Šimoník, J. *J. Appl. Polym. Sci.* **2007**, *106*, 926.
12. Cui, L.; Khramov, D. M.; Bielawski, C. W.; Hunter, D. L.; Yoon, P. J.; Paul, D. R. *Polymer* **2008**, *49*, 3751.
13. Gelfer, M. Y.; Burger, C.; Chu, B.; Hsiao, B. S.; Drozdov, A. D.; Si, M.; Rafailovich, M.; Sauer, B. B.; Gilman, J. W. *Macromolecules* **2005**, *38*, 3765.
14. Fornes, T. D.; Yoon, P. J.; Paul, D. R. *Polymer* **2003**, *44*, 7545.
15. Narkhede, J. S.; Shertukde, V. V. *J. Appl. Polym. Sci.* **2010**, *119*, 1067.
16. Avalos, F.; Ortiz, J. C.; Zitzumbo, R.; López-Manchado, M. A.; Verdejo, R.; Arroyo, M. *Appl. Clay Sci.* **2009**, *43*, 27.
17. Calderon, J. U.; Lennox, B.; Kamal, M. R. *Appl. Clay Sci.* **2008**, *40*, 90.
18. Ngo, H. L.; LeCompte, K.; Hargens, L.; McEwen, A. *Thermochim. Acta* **2000**, *357–358*, 97.
19. Cui, L.; Bara, J. E.; Brun, Y.; Yoo, Y.; Yoon, P. J.; Paul, D. R. *Polymer* **2009**, *50*, 2492.
20. Stoeffler, K.; Lafleur, P. G.; Denault, *J. Polym. Eng. Sci.* **2008**, *48*, 1449.
21. Awad, W. *Thermochim. Acta* **2004**, *409*, 3.
22. Davis, C. H.; Mathias, L. J.; Gilman, J. W.; Schiraldi, D. A.; Shields, J. R.; Trulove, P.; Sutto, T. E.; Delong, H. C. *J. Polym. Sci. Part B: Polym. Phys.* **2002**, *40*, 2661.
23. Gilman, J. W.; Awad, W. H.; Davis, R. D.; Shields, J.; Harris, R. H.; Davis, C.; Morgan, A. B.; Sutto, T. E.; Callahan, J.; Trulove, P. C.; Delong, H. C. *Chem. Mater* **2002**, *14*, 3776.
24. Pogodina, N. V.; Cerclé, C.; Avérous, L.; Thomann, R.; Bouquey, M.; Muller, R. *Rheol. Acta* **2008**, *47*, 543.
25. Fenouillot, F.; Cassagnau, P.; Majeste, J. C. *Polymer* **2009**, *50*, 1333.
26. Van Krevelen, D. Properties of Polymers; Elsevier: Amsterdam, **1976**.
27. Fedors, R. F. *Polym. Eng. Sci.* **1974**, *14*, 147.
28. Hansen, C. M.; Wallström, E. *J. Adhes.* **1983**, *15*, 275.
29. Mark, J. Physical Properties of Polymers Handbook; Springer: New York, **2007**.
30. Wu, S. Polymer Interface and Adhesion; Dekker, M.: New York, **1982**.
31. Yousfi, M.; Soulestin, J.; Vergnes, B.; Lacrampe, M.-F.; Krawczak, P. *Macromol. Mater. Eng.* DOI: 10.1002/mame.201200138
32. Gelfer, M.; Song, H.; Liu, L.; Hsiao, B.; Chu, B.; Rafailovich, M.; Si, M.; Zaitsev, V. *J. Polym. Sci. Part B: Polym. Phys.* **2003**, *41*, 44.
33. Shah, R.; Krishnaswamy, R.; Takahashi, S.; Paul, D. *Polymer* **2006**, *47*, 6187.
34. Serpe, G.; Jarrin, J.; Dawans, F. *Polym. Eng. Sci.* **1990**, *30*, 553.
35. Dharaiya, D.; Jana, S. C. *Polymer* **2005**, *46*, 10139.
36. Retolaza, A.; Eguiazabal, J.; Nazabal, *J. Polym. Eng. Sci.* **2002**, *42*, 2072.
37. Wang, Y.; Gao, J.; Ma, Y.; Agarwal, U. *Compos B* **2006**, *37*, 399.
38. Cervantes-Uc, J.; Cauich-Rodriguez, J.; Vazquez-Torres, H.; Garfias Mesias, L.; Paul, D. *Thermochim. Acta* **2007**, *457*, 92.

39. Chiu, F.-C.; Yen, H.-Z.; Chen, C.-C. *Polym. Test.* **2010**, *29*, 706.
40. Hobbs, S.; Dekkers, M.; Watkins, V. *Polymer* **1988**, *29*, 1598.
41. Guo, H. F.; Packirisamy, S.; Gvozdic, N. V.; Meier, D. *J. Polymer* **1997**, *38*, 785.
42. Horiuchi, S.; Matchariyakul, N.; Yase, K.; Kitano, T. *Macromolecules* **1997**, *30*, 3664.
43. Le Corroller, P.; Favis, B. D. *Polymer* **2011**, *52*, 3827.
44. Ohishi, H. *J. Appl. Polym. Sci.* **2004**, *93*, 1567.
45. Wang, D.; Li, Y.; Xie, X.-M.; Guo, B.-H. *Polymer* **2011**, *52*, 191.
46. Virgilio, N.; Desjardins, P.; L'Espérance, G.; Favis, B. D. *Macromolecules* **2009**, *42*, 7518.
47. Virgilio, N.; Marc-Aurèle, C.; Favis, B. D. *Macromolecules* **2009**, *42*, 3405.
48. Taguet, A.; Huneault, M. A.; Favis, B. D. *Polymer* **2009**, *50*, 5733.
49. Girifalco, L.; Good, R. *J. Phys. Chem.* **1957**, *61*, 904.
50. Kusmono, K. *Express Polym. Lett.* **2008**, *2*, 655.